# Synthetic peptides, nucleic acids and molecular probes to study ADP-Ribosylation

Voorneveld, J.

# Chapter 8

## Olaparib-Based Photoaffinity Probes for PARP-1 Detection in Living Cells

# Introduction

One of the crucial steps in the repair of DNA double-strand breaks is ADP-ribosylation of chromatin,[1–6] a process driven by several members of the PARP family.[7–9] This family of transferases represents clinically relevant target proteins for drugs directed at tumors that are deficient in their DNA repair.[10,11] The ability to monitor PARPs *in vivo* is necessary in order to study the processes of the drug-target engagement and pharmacokinetics. One method of accomplishing this involves small molecule probes, which are capable to specifically and covalently bind to their target enzymes in living cells and in tissues. These probes have been developed for various classes of enzymes[12–16] and used in successful studies involving *in vivo* protein detection and quantification. One way to attain such a probe is to convert a known reversible enzyme inhibitor into a covalent probe suitable for affinity-based protein profiling (AfBPP).[16–19] AfBPP probes consist of a recognition element that reversibly interacts with the target of interest, to which a photoreactive group and bioorthogonal ligation handle are installed, without affecting the affinity of the parent structure. Irradiation by UV light activates the photoreactive group, creating a reactive intermediate which can form a covalent bond between the probe and the target protein in a process called photo-affinity labeling (PAL).[19–21] The bioorthogonal ligation handle is used to couple a reporter group, e.g. a fluorophore for in-gel analysis or a biotin for affinity enrichment with subsequent tandem mass spectrometry in chemical proteomics. This chapter presents such a covalent probe for the detection of PARP-1 in live cells using AfBPP (Figure 1). Prior work on the detection of PARP was focused solely on non-covalently binding molecules with the aim of either off-target finding[22,23] or *in vivo* imaging.[24,25] Therefore attention was directed to design, synthesize and biologically validate a PARP-1-selective photoaffinity probe for use in the standard proteomics protocols. Such well-established workflows make use of UV-induced PAL through a diazirine tag and copper-catalyzed alkyne-azide cycloaddition (CuAAC) that enable the pull-down of the protein for subsequent analysis by standard mass-spectrometry methods.

In this chapter, the design, synthesis and biological evaluation and validation of a PARP-1-selective photoaffinity probe for the use of chemical proteomics is presented. Such well-established workflows make use of UV-induced PAL through a diazirine tag and CuAAC that enable the pull-down of the protein for subsequent analysis by mass-spectrometry methods.

The clinical PARP inhibitor olaparib was chosen as the starting point for the design of the recognition element of photoaffinity probes **3** and **6** (Scheme 1), because it inhibits PARP-1 and PARP-2 with a nanomolar potency and shows exceptional selectivity over other cellular targets.[23,26,27] For PAL, a plethora of photoreactive groups have been

reported.[28] In order to limit the interference of the tag with the activity and selectivity of the probes, the compact diazirine-alkyne linkers **2** and **5** developed by Li *et al.*[29] were opted. Placement of the photoreactive group is of importance since it must be close to the peptide backbone of the protein of interest, yet not interfere with the affinity of the probe by steric hindrance. The nitrogen atom of the piperazine moiety distal from the phtalazinone substructure of olaparib is known to tolerate a wide range of modifications.[27,30] With this in mind, the photoaffinity tag can be attached to this nitrogen to minimize its influence on the binding efficiency to PARP-1, giving the design of probe **3**. A second, simplified probe **6**, in which the piperazine bridge was removed and the diazirine-alkyne tag was attached directly to benzylphtalazinone core of the olaparib structure was also synthesized.

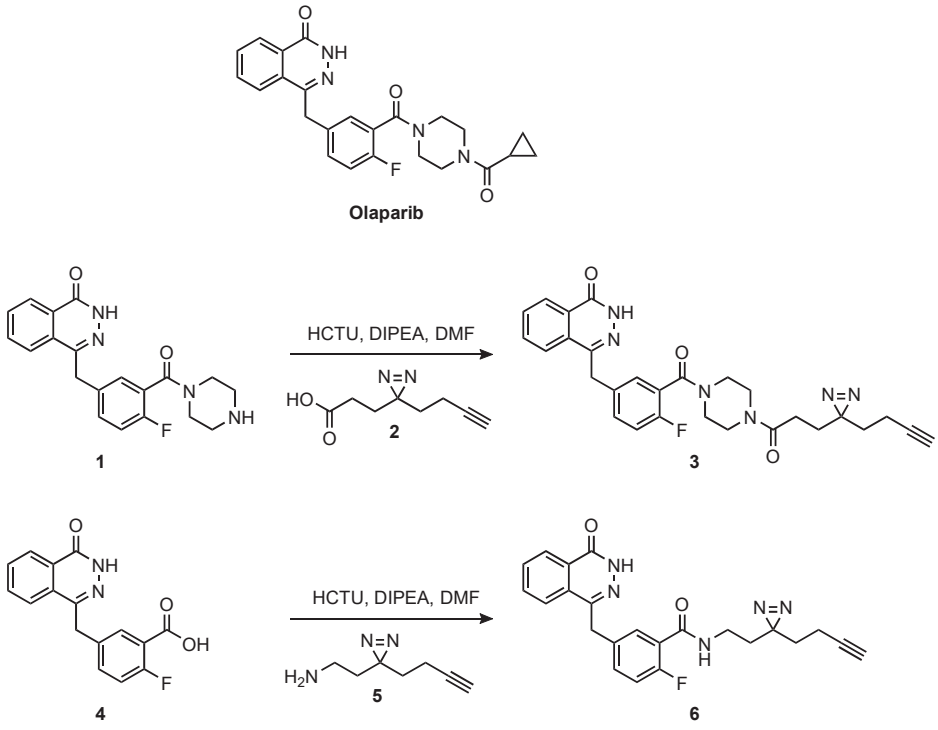


**Scheme 1.** Structure of olaparib and the synthesis of the probes **3** and **6** derived from olaparib. Yields obtained are 33% for **3** and 75% for **6**.

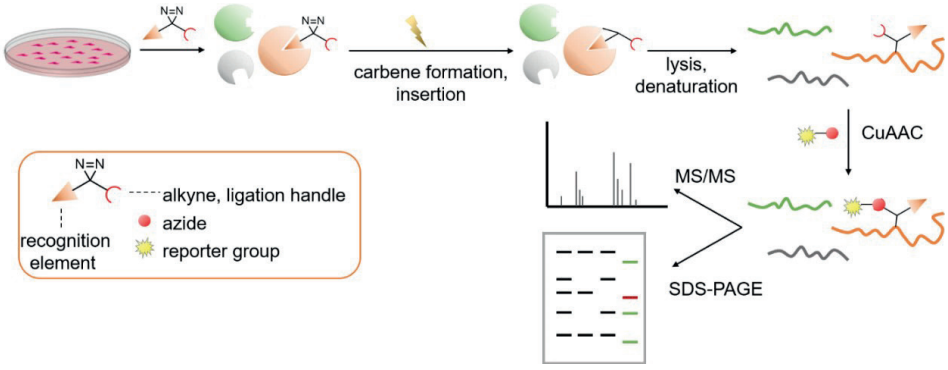


**Figure 1.** Schematic overview of AfBPP. After cells are treated with probe, irradiation at 350 nm leads to activation of the diazirine group, forming a highly reactive carbene that can rapidly insert into nearby N-H, O-H or C-H bonds. Protein extraction is done by cell lysis under denaturating conditions. Reporter or affinity handles are introduced by CuAAC click chemistry. Proteins are analyzed by SDS-PAGE and/or western blot analysis or by affinity purification, digested to peptides and LFQ proteomics analysis.



## Results and discussion

Preparation of the probes was done via the HCTU-mediated condensation of either commercially available **1** or known compound **4**[24,27] with the linkers **2** and **5** respectively (Scheme 1). With the AfBPs **3** and **6** in hand, their ability to bind PARP covalently via PAL in live cells was tested on human B-cell-derived Raji cell line. Raji cells were chosen as the model because they have been previously used to study PARP[31] and have an advantageous nucleus to cytoplasm ratio that maximizes the PARP abundance. The cells were incubated with probes **3** or **6** (10 µM) and irradiated with UV light for 30 minutes to ensure complete activation of the diazirine and covalent labeling of PARP. During irradiation, the cells were cooled to 4 °C to counteract the heat generated from the irradiation. The cells were then harvested and lysed. Probe-bound proteins were ligated to azide-containing fluorophore AlexaFluor 647-$N_3$ under CuAAC conditions and further processed for in-gel fluorescence analysis. The gel revealed a fluorescent band at the expected height of PARP-1 around 116 kDa (Figure 2, lane 3), which was probe-dependent as cells treated with vehicle (lane 2) revealed no labeling. To further show probe-specific labeling, the UV irradiation step was omitted (lane 1) yielding no signal, showing that the observed labeling is UV-dependent rather than circumstantial activation.

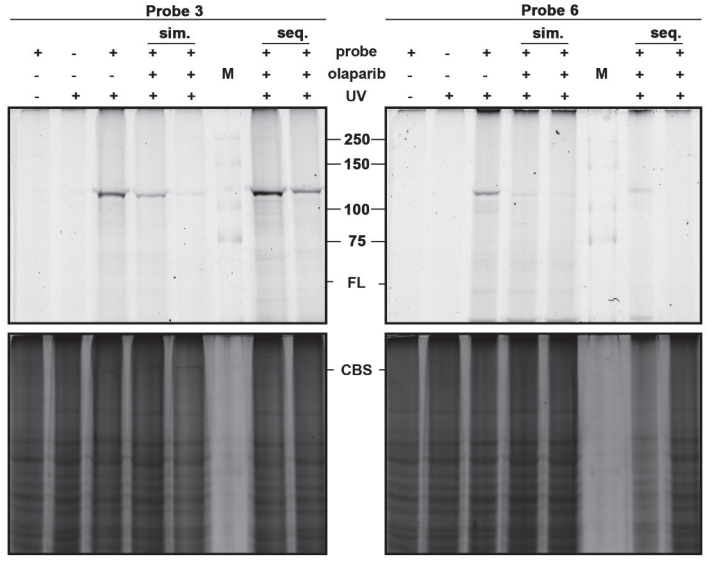


**Figure 2.** SDS-PAGE analysis of Raji cells exposed to probes **3** (left) and **6** (right) (10 μM) and no UV control. sim: simultaneous incubation with 1:1 (10 μM olaparib, 10 μM probe) or 5:1 (50 μM olaparib, 10 μM probe) ratio. seq: sequential incubation with olaparib, wash and probe at 1:1 ratio or 2:1 olaparib:probe ratio. FL: fluorescence channel. CBS: Coomassie blue staining for loading control of the gel in the upper panel. M: protein ladder

As an additional control, the gel used for in-gel fluorescence readout was analyzed by western blot with an anti-PARP-1 antibody confirming the fluorescent bands to be PARP-1 (Figure 3, bottom panel). To further verify the target, the experiments were repeated but the click reaction was performed with *N*-(3-azidopropyl)biotinamide, providing a handle to perform a pull-down with streptavidin. Probe-bound proteins from the lysates were enriched on streptavidin-coated beads and analyzed with SDS-PAGE followed by WB analysis with the anti-PARP-1 antibody to ascertain that the enriched protein is PARP-1 (data not shown). Having verified that probes **3** and **6** were able to label PARP in a UV-dependent, covalent manner, the binding site of the probe was investigated. If the probe retains the binding mode of the parent structure, labeling should be outcompeted by addition of olaparib. The probes and olaparib were incubated simultaneously in a 1:1 ratio after which a decrease of band intensity was observed (Figure 2, lane 4). After increasing the amount of olaparib to a 5:1 drug/probe ratio, labeling by the probe was abolished (lane 5). Interestingly, in a sequential competition experiment where the cells were first incubated with olaparib, washed, and then incubated with the probes in a 1:1 ratio, no apparent competition was observed (lane 7). Repeating the experiment with a 2:1 drug/probe ratio appeared to slightly increase competition of the probes (lane 8) but proved not as effective as simultaneous competition. This effect might be due to rapid dissociation of olaparib from the PARP-binding pocket during the washing step.

Next, attention was turned to demonstrate the ability of the probe to bind PARP in conditions frequently encountered in the field of ADP-ribosylation research. Treatment of cells with $H_2O_2$ generates DNA damage, which results in double strand breaks and subsequent activation of PARP. Therefore, Raji cells were treated with the probes as before but with addition of $H_2O_2$ during incubation. The addition of this oxidizing agent neither changed the ability of the probes to label PARP nor the efficiency of the labeling (Figure 3), suggesting that olaparib is able to bind PARP in the presence of extensive DNA-damage and appears consistent with previously reported findings.[22]

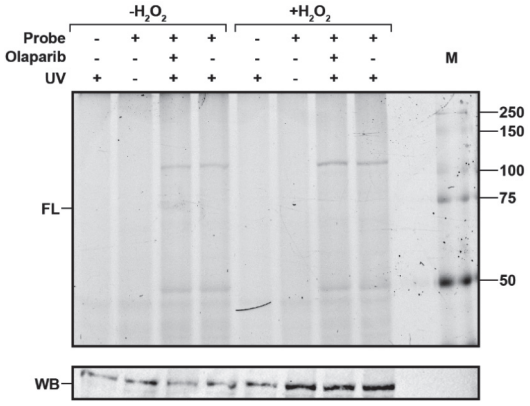


**Figure 3.** SDS-PAGE analysis with fluorescent imaging (FL) or western blot (WB) detection of Raji cell lysate either exposed or not exposed to $H_2O_2$ and probe 3, no-UV control, without or in sequential competition with olaparib (1:1 olaparib:probe ratio). WB: loading control and PARP1 detection of the gel in the upper panel by western blot analysis with a rabbit anti-PARP1 antibody. M: protein ladder

To identify and quantify the bands seen by SDS-PAGE and western blot analysis, an LC-MS/MS based label-free quantification (LFQ) method was used.[15] The results, depicted in Figure 4, show that PARP-1 is significantly UV-enriched by probe **3** indicating that the observed band at 116 kDa can be attributed to PARP-1 (Figures 4A and B). Competition analysis of significantly UV-enriched proteins shows PARP-1 is outcompeted by olaparib (Figure 4D) strongly indicating that the probe binds in the same protein pocket as olaparib. Several other proteins were selectively enriched by the probe upon UV irradiation having a nucleic acid binding motif as common feature, indicating that the probe targets these proteins possibly by their nucleic acid binding or perhaps by the presence of the diazirine group (Figure 4C).[32] PARP-1 was not significantly UV-enriched by probe **6** (data not shown) which agrees with the in-gel fluorescence data for this probe that showed fainter bands for PARP-1 compared with the background. Apparently, removal of the piperazine ring diminishes the binding affinity of probe **6** to PARP-1.

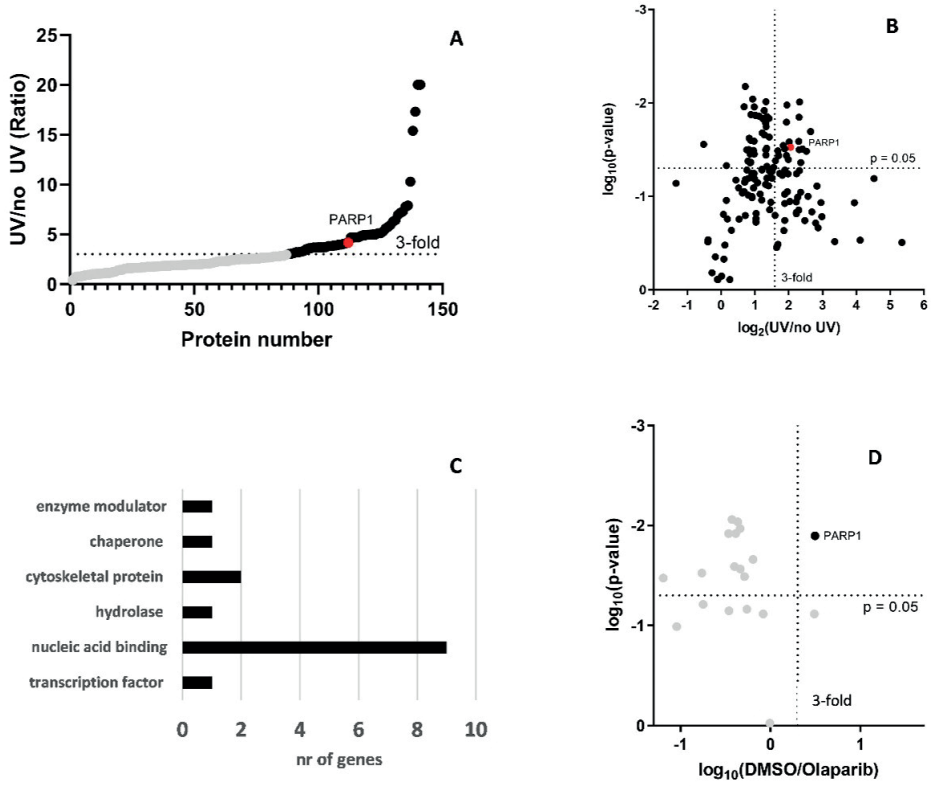


**Figure 4.** LFQ proteomics analysis of probe **3** in living Raji cells of proteins with at least 2 unique peptides. **A:** Waterfall plot of UV enrichment by probe **3** of proteins identified in the proteomics analysis, proteins showing >3-fold UV enrichment are in black. **B:** Volcano plot of UV enrichment of proteins by probe **3.** PARP-1 is marked in red. **C:** Significantly UV-enriched proteins sorted with the gene function analysis module of the PANTHER classification system (v.14.0) software.[33] **D:** Competition analysis of significantly UV-enriched probe targets, proteins outcompeted >3-fold by olaparib preaddition with a p-value < 0.05 using a Student's t-test are in black.

# Conclusion

The design and synthesis of two synthetically accessible olaparib-based photoaffinity probes (**3** and **6**) for PARP-1 detection in living cells is presented in this chapter. Evidence for the efficacy of the probes is shown and a detailed protocol for application of these probes is provided therewith. Both **3** and **6** proved to be stable under oxidative conditions often employed for PARP activation while probe **3** was successfully used to label PARP-1 selectively in a live cell model and to detect its presence by in-gel fluorescence and LFQ LC-MS/MS methods.

# Experimental section

**General synthetic procedures**

All reagents were used as received unless stated otherwise. Solvents used in synthesis were dried and stored over 4Å molecular sieves, except for MeOH and ACN which were stored over 3Å molecular sieves. Triethylamine (TEA) and diisopropylethylamine (DIPEA) were stored over KOH pellets. Column chromatography was performed on silica gel 60 Å (40-63 µm, Macherey-Nagel). TLC analysis was performed on Macherey-Nagel aluminium sheets (silica gel 60 $F_{254}$). TLC was used to visualize compounds by UV at wavelength 254 nm and by spraying with either cerium molybdate spray (25 g/L $(NH_4)_6Mo_7O_{24}$, 10 g/L $(NH_4)_4Ce(SO_4)_4{\cdot}H_2O$ in 10% $H_2SO_4$ water solution) or $KMnO_4$ spray (20 g/L $KMnO_4$ and 10 g/L $K_2CO_3$ in water) followed by charring at c.a. 250 °C. LC-MS analysis was performed on a Finnigan Surveyor HPLC system with a Nucleodur C18 Gravity 3 µm 50 x 4.60 mm column (detection at 200-600 nm) coupled to a Finnigan LCQ Advantage Max mass spectrometer with ESI or coupled to a Thermo LCQ Fleet Ion mass spectrometer with ESI. The method used was 10→90% 13.5 min (0→0.5 min: 10% MeCN; 0.5→8.5 min: 10% to 90% MeCN; 8.5→ 11 min: 90% MeCN; 11→13.5 min: 10% MeCN). NMR spectra were recorded on a Bruker AV-500 NMR. Chemical shifts (δ) are given in ppm relative to tetramethyl silane as internal standard. Coupling constants (*J*) are given in Hz. All given $^{13}$C-APT spectra are proton decoupled.



**4-(3-(4-(3-(3-(but-3-yn-1-yl)-3*H*-diazirin-3-yl)propanoyl)piperazine-1-carbonyl)-4-fluorobenzyl) phthalazin-1(2*H*)-one (3)**

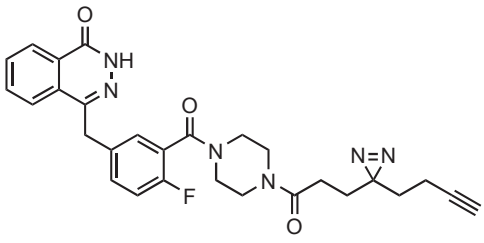

Compound **1** (38 mg, 0.10 mmol, 1.0 eq.), compound **2** (19 mg, 0.11 mmol, 1.1 eq.) and DIPEA (40 µL, 0.23 mmol, 2.2 eq.) were dissolved in DMF (1 mL). HCTU (47 mg, 0.11 mmol, 1.1 eq.) was added and the reaction was stirred at room temperature for 1.5 h. TLC showed full conversion, $R_f$ = 0.73; DCM:MeOH=9:1 + three drops of TEA. The reaction was quenched by the addition of water and transferred into a separatory funnel. The water layer was extracted with EtOAc and the combined organic layers were dried over $MgSO_4$, filtered and concentrated *in vacuo*. The crude product was purified by silica gel column chromatography (1 -> 5% MeOH in DCM) to obtain the title compound **3** (17 mg, 0.033 mmol, 33%) as a white solid. **$^1$H-NMR** (500 MHz, $CDCl_3$) δ 12.12 – 11.89 (m, 1H, H-9), 8.48 (dd, J = 6.3, 3.2 Hz, 1H, H-6), 7.86 – 7.61 (m, 3H, H-1, H-2, H-3), 7.41 – 7.32 (m, 2H, H-14, H-18), 7.04 (td, J = 8.8, 2.4 Hz, 1H, H-15), 4.31 (s, 2H, H-12), 4.00 – 3.15 (m, 8H, H-22, H-23, H-25, H-26), 2.12 (t, J = 7.6 Hz, 1H, H-38), 2.07 – 1.92 (m, 4H, H-31, H-33), 1.88 (q, J = 7.4 Hz, 2H, H-36), 1.74 – 1.59 (m, 2H, H-29). **$^{13}$C-NMR** (126 MHz, $CDCl_3$) δ 169.8 + 169.7 (C-28, rotamers), 165.3 + 165.0 (C=O amide, rotamers), 161.1 (C-10), 157.9 + 156.0 (C-16, *J* = 239 Hz), 145.5 (C-7), 134.5 + 134.5 (C-13, *J* = 5.0 Hz), 133.6 (C-1/2/3), 131.8 + 131.8 (C-14, *J* = 7.5 Hz), 131.6 (C-1/2/3), 129.5 (C-4), 129.4 + 129.2 (C-18, rotamers), 128.2 (C-5), 127.1 (C-6), 125.0 (C-1/2/3), 123.6 + 123 (C-17, *J* = 17.5 Hz), 116.3 + 116.1 and 116.2 + 116.0 (C-15, *J* = 22.5 Hz) , 82.7 (C-37), 69.3 (C-38), 47.0 + 46.7 + 45.5 + 45.0 + 42.1 + 41.9 (C-22/23/25/26), 37.7 + 37.6 (C-12), 32.5 (C-29), 27.9 (C-31/C-33) 27.8 (C-31/C-33), 13.3 (C-36). **LC-MS:** 10 -> 90% B in A, Rt = 6.24. **HRMS:** $[C_{28}H_{27}FN_6O_3 + H]^+$: 515.2194 found, 515.2201 calculated

**N-(2-(3-(but-3-yn-1-yl)-3H-diazirin-3-yl)ethyl)-2-fluoro-5-((4-oxo-3,4-dihydrophthalazin-1-yl)methyl)benzamide (6)**

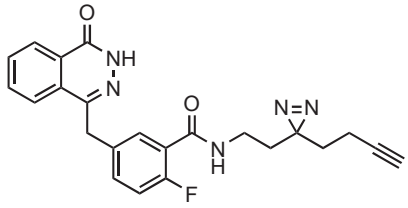

Compound **4** (60 mg, 0.20 mmol, 1.1 eq.), compound **5** (25 mg, 0.18 mmol, 1.0 eq.) and DIPEA (70 µL, 0.40 mmol, 2.2 eq.) were dissolved in DMF (1.5 mL). HCTU (83 mg, 0.20 mmol, 1.1 eq.) was added and the reaction was stirred for 16 h at room temperature. The reaction was quenched by the addition of water and transferred into a separatory funnel. The water layer was extracted with EtOAc and the combined organic layers were dried over $MgSO_4$, filtered and concentrated *in vacuo*. The crude product was purified by silica gel column chromatography (2->20% MeOH in DCM) to obtain the title compound **6** (57 mg, 0.14 mmol, 75%) as a white solid. **$^1$H NMR** (500 MHz, $CDCl_3$) δ 11.27 (s, 1H, H-9), 8.55 – 8.39 (m, 1H, H-6), 8.09 (dd, *J* = 7.4, 2.5 Hz, 1H, H-18), 7.81 – 7.70 (m, 3H, H-1, H-2, H-3), 7.37 (ddd, *J* = 8.3, 4.8, 2.5 Hz, 1H, H-14), 7.06 (dd, *J* = 11.6, 8.5 Hz, 1H, H-15), 6.87 (dt, *J* = 12.1, 5.7 Hz, 1H, H-21), 4.33 (s, 2H, H-12), 3.34 (q, *J* = 5.5 Hz, 2H, H-23), 2.03 (td, *J* = 7.3, 2.6 Hz, 2H, H-27), 1.99 (t, *J* = 2.6 Hz, 1H, H-29), 1.82 (t, *J* = 6.8 Hz, 2H, H-24), 1.69 (t, *J* = 7.3 Hz, 2H, H-26). **$^{13}$C NMR** (126 MHz, $CDCl_3$) δ 163.3 + 163.3 (C-20), 160.9 (C-10), 160.7 + 158.7 (C-16, *J* = 246 Hz), 145.8 (C-7), 134.4 + 134.4 (C-13, *J* = 2.5 Hz), 133.8 (C1/2/3), 133.5 + 133.5 (C-14, *J* = 8.8 Hz), 132.0 + 132.0 (C-18, *J* = 2.5 Hz), 131.6 (C1/2/3), 129.6 (C-4), 128.4 (C-5), 127.2 (C-6), 125.2 (C1/2/3), 121.0 + 120.9 (C-17, *J* = 11 Hz), 116.8 + 116.6 (C-15, *J* = 25 Hz), 82.7 (C-28), 69.5 (C-29), 37.9 (C-12), 35.0 (C-23), 32.6 (C-24), 32.3 (C-26), 13.3 (C-27). **LC-MS:** 10 -> 90% B in A, Rt = 6.37. **HRMS:** $[C_{23}H_{20}FN_5O_2 + H]^+$: 418.1668 found, 418.1674 calculated.

**Cell culture**

Raji cells were cultured in phenol-red free RPMI-1640 medium buffered with sodium bicarbonate (Sigma-Aldrich) and freshly supplemented with new born calf serum (NBS, Hyclone), Glutamax, penicillin and streptomycin (200 µg/mL each, Duchefa) at 37°C in a humidified incubator with 7% $CO_2$. Phenol red was excluded from the medium to prevent UV light quenching by the pH indicator. Cells were growing happily and were passaged twice every week allowing for growth from 0.5 to 2-3 x $10^6$ per mL in T175 flasks supplied with 100 mL fresh medium. For each experiment, 150 x $10^6$ of logarithmically growing cells in 75 mL conditioned cell culture medium were seeded in T175 flasks and treated with 75 µL $H_2O$ (control) or 75 µL 500 mM $H_2O_2$ (500 µM final) to induce double strand breaks for 30 minutes in the incubator. Cells were pelleted by centrifugation (5 minutes, 200 *g*), the supernatant was removed, the cell pellet was washed by trituration in 20 mL colourless RPMI-1640 medium supplemented with Glutamax (RPMI-g), spun down (5 minutes, 200 *g*) after which the cells were suspended in 3 mL RPMI-g and divided in 3 equal parts in 2 mL Eppendorf tubes.

**Olaparib treatment**

The cells were treated with 10 µM olaparib (2 mM in DMSO, Cayman Chemicals) or vehicle (5 µl of DMSO) and were incubated for 1 h at 37°C with shaking at 600 rpm. In case of sequential olaparib competition, the cells were pelleted, suspended in 2 mL RPMI-g, pelleted again, suspended in 1 mL RPMI-g containing 10 µM probe **3** or **6** or vehicle (5 µL DMSO) and were incubated for 2 h at 37 °C with shaking at 600 rpm. In case of simultaneous olaparib competition, µL 10 µM probe **3** or **6** or vehicle (5 µL DMSO) was added and cells were incubated for 2 h at 37°C with shaking at 600 rpm. The maximum DMSO concentration was 1%, probes were at 10 µM and olaparib was at 10 and 50 µM (1:1 or 5:1 of olaparib:probe ratios) end concentrations. After the incubation, cells were pelleted by centrifugation (5 minutes, 200 *g*), washed with 2 mL RPMI-g by pelleting (5 minutes, 200 *g*) and trituration in fresh RPMI-g, washed with 2 mL phosphate buffered saline (PBS) at 37 °C, washed with 2 mL ice cold PBS and suspended in 1 mL ice cold PBS.

**UV-irradiation**

Cells were plated on a 35 mm Petri dish and irradiated with 350 nm UV light for 30 minutes on a metal platform cooled at 2 °C (Caprotec box). The Caprobox contains 3 x 8.6 Watt UV lamps (Philips PL-S 9W BLB 2-Pin) that cover a surface of 0.01 $m^2$ and delivers 15.5 kJ in 30 minutes. A systematic variation to determine the optimal amount of UV light exposure was not performed, however pilot experiments with 10 and 20 minutes exposure yielded less pronounced PARP bands (data not shown). For no-UV controls, cells were plated on Petri dishes and incubated on ice for 30 minutes.

**Cell lysis**

Cells were collected, pelleted by centrifugation (4 °C, 5 minutes, 200 *g*), and the supernatant was removed. To prevent unwanted post-lysis processing of PARP and loss in reporter tag installation efficiency, the cell lysis and the CuAAC click chemistry were performed under denaturing conditions. Pilot experiments with lysis and CuAAC click in native protein environments (50 mM HEPES pH 7.4, 150 mM NaCl, protease inhibitors) showed less pronounced PARP bands after SDS-PAGE analysis, while native lysis followed by denaturation with 8 M urea prior to the click chemistry showed stronger bands (data not shown). The cell pellet was lysed under denaturing conditions by adding 300 µL lysis buffer (8 M urea, 10 mM HEPES, pH 7.4) and trituration until a highly viscous solution was reached due to the released DNA. The lysates were left on ice for 15 minutes, followed by DNA shearing with 5 pulses of 5 seconds by tip sonication on ice. Cell debris (small translucent pellet) was removed by centrifugation (4 °C, 15 minutes, 20.000 *g*), the supernatant transferred to a new tube and the protein concentration ranged from 8 — 15 µg/µL as determined with the Bradford colorimetric assay using a calibration curve of bovine serum albumin (BSA).



**Copper catalysed click reaction**

75 µg of protein (5 µL lysate) was mixed with 5 µL lysis buffer and 10 µL click cocktail and allowed to react at room temperature (RT) for 1 h in the dark. The click cocktail was made by first mixing 8 µL aq. $CuSO_4$ (100 mM) and 8 µl aq. sodium ascorbate (1 M) that resulted in a colour change from light blue to orange/brown due to reduction of $Cu^{2+}$ to $Cu^{+}$. Addition of 8 µL THPTA (100 mM in DMSO) ligand that coordinates and stabilises the $Cu^{+}$ species made the solution turn colourless. To prevent side reaction with amines of arginine residues, 8 µL aq. aminoguanidine (1 M) was added followed by 233 µL HEPES (100 mM, pH 7.4) and 0.8 µL AlexaFluor 647 azide (2 mM, Thermo Fisher Scientific) for fluorescent detection or diazo-biotin azide (2 mM, Click Chemistry Tools) for western blot analysis with Streptavidin-AlexaFluor 647 (Thermo Fisher Scientific) or affinity purification with MyOne C1 beads (Thermo Fisher Scientific). 7 µL 4X concentrated Laemmli sample buffer (SB) was added followed by heating at 95 °C for 5 minutes.

**SDS PAGE analysis**

Proteins were separated on a 1.5 mm, 10% SDS-PAGE gel at 100 V for 10 min and 130 V for another 3 hours, after which fluorescent signal was recorded on a Chemidoc MP system Bio-Rad). For reproducible PARP1 results, a minimum of 50 µg total protein loading per lane is necessary which justifies the use of the 1.5 mm thickness gels. In some cases, we have experienced unreproducible background staining possibly caused by the excess click cocktail reagents (data not shown). To eliminate background staining and clean the sample, a chloroform/methanol protein precipitation step between the click and SB steps was performed. After the click reaction, 80 µl lysis buffer was added followed by 400 µl methanol and vigorous mixing, then 100 µl chloroform, vigorous mixing and 300 µl water and vigorous mixing. Water addition leads to phase separation and with proteins precipitating out of solution as

white particles. Centrifugation at 10.000 g for 5 minutes affords a 3-layer system with water on top, organic layer at the bottom and a white protein interface as a thin film in the middle. The water layer is removed and 300 µl methanol is added followed by gentle mixing. Centrifuge at 10.000 g for 5 minutes to get the protein film at the bottom of the tube, remove the organic solvent completely and dry the tube for exactly 5 minutes at air in the fume hood. The protein film was solubilised in 30 µl 1x SB and heating at 95 °C for 5. This cleaning step is down scalable to protein amounts of minimum of 40 µg, less protein makes visibility of the protein film quite difficult and does not cause significant loss of PARP protein molecules. Coomassie served as loading control.

**Western blot analysis**

For PARP1 WB analysis, gels were first imaged by fluorescence followed by protein transfer to nitrocellulose membranes (Bio-Rad) using the high MW protocol (10 minutes at 2.5A, 25V) on a Trans-blot turbo transfer system (Bio-Rad) The precision plus dual color protein standard (Bio-Rad) was diluted 10x with 1xSB and 2 µL were loaded to assess the running of the gel and the electro transfer of the proteins to the nitrocellulose membranes. The membranes were washed with water and TBST (Tris buffered saline, 0.1% Tween 20) and subsequently blocked using 5% non-fat milk in TBST (30 minutes). To this, 4 µL of a rabbit-anti-PARP1 (9542, Cell Signalling Technology) antibody (1:2500 dilution) was added and incubated overnight at 4 °C. The blot was washed with 20 mL TBST (4X, 5 minutes), blocked again for 30 minutes in 10 mL 5% milk, and rolled with 5 µL (1:2000) secondary anti-rabbit IgG, HRP-linked antibody (7074, Cell Signalling Technology) for 1 h at rt. The membrane was washed with 20 mL TBST(4X, 5 minutes), TBS, water and subsequently imaged with Clarity max western ECL substrate (Bio-Rad) on the Chemidoc MP system. For biotin visualisation, the western blot procedure for PARP1 was used with several modifications. The blocking solution was 3% BSA in TBST, hybridisation with Streptavidin-AlexaFluor647 (1:2000) was used to tag biotinylated proteins for 1 h at room temperature or overnight at 4 °C.

**Label free quantification by LC-MS/MS**

For label-free quantification by LC-MS/MS-based proteomics (LFQ), biotin-$N_3$ was installed by CuAAC in 1 mg of protein in 100 µL lysis buffer reacted with 50 µL click cocktail for 1 h at RT in the dark followed by Bligh&Dyer precipitation to remove excess reagents. The protein film was taken in 100 µL 1% SDS/100 mM HEPES pH 7.4, allowed 30 minutes to dissolve with shaking at 600 rpm at RT, centrifuged at 20.000 g for 5 minutes at RT to remove particles and the solution transferred to a new tube. Disulfide bridges were reduced by addition of 5 µL 100 mM DTT (5 mM end concentration) for 30 minutes at 37°C and alkylated with 5 µL 400 mM iodoacetamide (20 mM end concentration) for 30 minutes at rt in the dark. Excess reagents were removed by Bligh&Dyer precipitation and the protein film was dispersed in 50 µL 2 % SDS/100 mM $NH_4HCO_3$ by vigorous vortexing. Stepwise dilution of 3 x 50 µl, 2 x 100 µl, 500 and 1000 µL pull down (PD) buffer (50 mM Tris pH7.4, 150 mM NaCl) followed by vigorous vortexing afforded a clear solution containing 0.05% SDS end concentration that is compatible with the streptavidin beads. After centrifugation at 20.000 g for 10 minutes to remove particles, the supernatant was transferred to a new tube. The pulldown was initiated by addition of 50 µL MyOne C1 streptavidin Dynabeads (Thermo Fisher Scientific) equilibrated in PD buffer and incubated for 1 h at RT or overnight at 4°C. After the incubation, the beads were collected for 2 minutes on the DynaMag (Thermo Fisher Scientific) and the supernatant was transferred to a new tube. The beads were washed with 2 × 500 µL of wash buffer I (4 M urea/50 mM $NH_4HCO_3$, 150 mM NaCl), 2 × 500 µL of wash buffer II (50 mM Tris pH = 7.4, 10 mM NaCl) and taken up in 200 µL on-bead digestion buffer (100 mM Tris pH 7.4, 10 mM NaCl, 1 mM $CaCl_2$, 2% MeCN in MilliQ water) followed by addition of 250 ng trypsin

(Promega). The beads were incubated at 37 °C overnight with shaking, collected on the DynaMag for 2 minutes and the supernatants containing the peptides were transferred to fresh tubes to which 5 µL of formic acid was added. Peptides were desalted using StageTips, concentrated to dryness, dissolved in 30 µL 96.9 % $H_2O$, 3% MeCN, 0.1% formic acid containing 10 fmol/µL enolase digest (Thermo Fisher Scientific) and 5 µL were analysed by nanoAcquity hyphenated to a Synapt G2Si mass spectrometer as previously described.[15] Peptide identification and LFQ was done by processing the raw data files with the Progenesis QIP software, proteins with at least 2 unique peptides were selected, normalised to enolase and the significance was determined with a Student's t-test and plotted versus the fold change for UV/no UV and with or without olaparib competition.

# References


[1] S. Messner, M. O. Hottiger, *Trends Cell Biol.* **2011**, *21*, 534–542.

[2] K. Ueda, A. Omachi, M. Kawaichi, O. Hayaishi, *Proc. Natl. Acad. Sci. U. S. A.* **1975**, *72*, 205–209.

[3] T. Boulikas, *Proc. Natl. Acad. Sci. U. S. A.* **1989**, *86*, 3499–3503.

[4] A. Huletsky, C. Niedergang, A. Fréchette, R. Aubin, A. Gaudreau, G. G. Poirier, *Eur. J. Biochem.* **1985**, *146*, 277–285.

[5] N. A. Berger, G. W. Sikorski, *Biochemistry* **1981**, *20*, 3610–3614.

[6] E. G. Miller, *BBA Sect. Nucleic Acids Protein Synth.* **1975**, *395*, 191–200.

[7] S. Messner, M. Altmeyer, H. Zhao, A. Pozivil, B. Roschitzki, P. Gehrig, D. Rutishauser, D. Huang, A. Caflisch, M. O. Hottiger, *Nucleic Acids Res.* **2010**, *38*, 6350–6362.

[8] S. L. Rulten, A. E. O. Fisher, I. Robert, M. C. Zuma, M. Rouleau, L. Ju, G. Poirier, B. Reina-San-Martin, K. W. Caldecott, *Mol. Cell* **2011**, *41*, 33–45.

[9] B. Lüscher, M. Bütepage, L. Eckei, S. Krieg, P. Verheugd, B. H. Shilton, *Chem. Rev.* **2018**, *118*, 1092–1136.

[10] C. J. Lord, A. Ashworth, *Science* **2017**, *355*, 1152–1158.

[11] N. Curtin, *Biochem. Soc. Trans.* **2014**, *42*, 82–88.

[12] N. Liu, S. Hoogendoorn, B. van de Kar, A. Kaptein, T. Barf, C. Driessen, D. V. Filippov, G. A. van der Marel, M. van der Stelt, H. S. Overkleeft, *Org. Biomol. Chem.* **2015**, *13*, 5147–5157.

[13] M. P. Baggelaar, H. den Dulk, B. I. Florea, D. Fazio, N. Bernabò, M. Raspa, A. P. A. Janssen, F. Scavizzi, B. Barboni, H. S. Overkleeft, M. Maccarrone, M. van der Stelt, *ACS Chem. Biol.* **2019**, *14*, 2295–2304.

[14] A. C. M. van Esbroeck, A. P. A. Janssen, A. B. Cognetta, D. Ogasawara, G. Shpak, M. van der Kroeg, V. Kantae, M. P. Baggelaar, F. M. S. de Vrij, H. Deng, M. Allarà, F. Fezza, Z. Lin, T. van der Wel, M. Soethoudt, E. D. Mock, H. den Dulk, I. L. Baak, B. I. Florea, G. Hendriks, L. De Petrocellis, H. S. Overkleeft, T. Hankemeier, C. I. de Zeeuw, V. Di Marzo, M. Maccarrone, B. F. Cravatt, S. A. Kushner, M. van der Stelt, *Science* **2017**, *356*, 1084–1087.

[15] E. J. van Rooden, B. I. Florea, H. Deng, M. P. Baggelaar, A. C. M. van Esbroeck, J. Zhou, H. S. Overkleeft, M. van der Stelt, *Nat. Protoc.* **2018**, *13*, 752–767.

[16] S. Pan, H. Zhang, C. Wang, S. C. L. Yao, S. Q. Yao, *Nat. Prod. Rep.* **2016**, *33*, 612–620.

[17] M. P. Baggelaar, P. J. P. Chameau, V. Kantae, J. Hummel, K. L. Hsu, F. Janssen, T. van der Wel, M. Soethoudt, H. Deng, H. den Dulk, M. Allarà, B. I. Florea, V. Di Marzo, W. J. Wadman, C. G. Kruse, H. S. Overkleeft, T. Hankemeier, T. R. Werkman, B. F. Cravatt, M. van der Stelt, *J. Am. Chem. Soc.* **2015**, *137*, 8851–8857.

[18] X. Yang, T. J. M. Michiels, C. de Jong, M. Soethoudt, N. Dekker, E. Gordon, M. van der Stelt, L. H. Heitman, D. van der Es, A. P. Ijzerman, *J. Med. Chem.* **2018**, *61*, 7892–7901.

[19] M. Soethoudt, S. C. Stolze, M. V. Westphal, L. van Stralen, A. Martella, E. J. van Rooden, W. Guba, Z. V. Varga, H. Deng, S. I. Van Kasteren, U. Grether, A. P. Ijzerman, P. Pacher, E. M. Carreira, H. S. Overkleeft, A. Ioan-Facsinay, L. H. Heitman, M. van der Stelt, *J. Am. Chem. Soc.* **2018**, *140*, 6067–6075.

[20] Z. Wang, Z. Guo, T. Song, X. Zhang, N. He, P. Liu, P. Wang, Z. Zhang, *ChemBioChem* **2018**, *19*, 2312–2320.

[21] M. Jouanneau, B. McClary, J. C. P. Reyes, R. Chen, Y. Chen, W. Plunkett, X. Cheng, A. Z. Milinichik, E. F. Albone, J. O. Liu, D. Romo, *Bioorganic Med. Chem. Lett.* **2016**, *26*, 2092–2097.

[22] K. S. Yang, G. Budin, C. Tassa, O. Kister, R. Weissleder, *Angew. Chemie - Int. Ed.* **2013**, *52*, 10593–10597.

[23] C. E. Knezevic, G. Wright, L. L. Remsing Rix, W. Kim, B. M. Kuenzi, Y. Luo, J. M. Watters, J. M. Koomen, E. B. Haura, A. N. Monteiro, C. Radu, H. R. Lawrence, U. Rix, *Cell Chem. Biol.* **2016**, *23*, 1490–1503.

[24] F. Zmuda, G. Malviya, A. Blair, M. Boyd, A. J. Chalmers, A. Sutherland, S. L. Pimlott, *J. Med. Chem.* **2015**, *58*, 8683–8693.

[25] T. Reiner, S. Earley, A. Turetsky, R. Weissleder, *ChemBioChem* **2010**, *11*, 2374–2377.
[26] E. D. Deeks, *Drugs* **2015**, *75*, 231–240.
[27] K. A. Menear, C. Adcock, R. Boulter, X. L. Cockcroft, L. Copsey, A. Cranston, K. J. Dillon, J. Drzewiecki, S. Garman, S. Gomez, H. Javaid, F. Kerrigan, C. Knights, A. Lau, V. M. Loh, I. T. W. Matthews, S. Moore, M. J. O'Connor, G. C. M. Smith, N. M. B. Martin, *J. Med. Chem.* **2008**, *51*, 6581–6591.
[28] P. Geurink, L. Prely, G. A. van der Marel, R. Bischoff, H. S. Overkleeft, *Photoaffinity Labeling in Activity-Based Protein Profiling*, **2011**.
[29] Z. Li, P. Hao, L. Li, C. Y. J. Tan, X. Cheng, G. Y. J. Chen, S. K. Sze, H. M. Shen, S. Q. Yao, *Angew. Chemie - Int. Ed.* **2013**, *52*, 8551–8556.
[30] E. Wahlberg, T. Karlberg, E. Kouznetsova, N. Markova, A. Macchiarulo, A. G. Thorsell, E. Pol, Å. Frostell, T. Ekblad, D. Öncü, B. Kull, G. M. Robertson, R. Pellicciari, H. Schüler, J. Weigelt, *Nat. Biotechnol.* **2012**, *30*, 283–288.
[31] W. Ma, C. J. Halweg, D. Menendez, M. A. Resnick, *Proc. Natl. Acad. Sci. U. S. A.* **2012**, *109*, 6590–6595.
[32] P. Kleiner, W. Heydenreuter, M. Stahl, V. S. Korotkov, S. A. Sieber, *Angew. Chemie - Int. Ed.* **2017**, *56*, 1396–1401.
[33] H. Mi, A. Muruganujan, X. Huang, D. Ebert, C. Mills, X. Guo, P. D. Thomas, *Nat. Protoc.* **2019**, *14*, 703–721.